University of Liège
Faculty of Applied Sciences

Perturbation Methods

Irrotational flow around cylinder with perturbation in boundary conditions

Professor: Vincent Denoël

Lucas Fuentes Valenzuela

Academic Year 2016-2017

Introduction

The present report presents a solution to the problem of irrotational flow around a cylinder with perturbed boundary conditions. More precisely, one wants to find an expression for the irrotational flow potential φ such that

$$\begin{aligned}&\Delta\varphi(r,\theta)=0,(r,\theta)\in[0;+\infty[\times[0;2\pi[,\\&\vec{n}\cdot\nabla\varphi=0,\ r=r_0(1+\varepsilon\cos(\theta)),\ \varepsilon>0,\\&\varphi(r\to+\infty)=Ur\cos(\theta).\end{aligned}$$

In the above equations, r_0 is the unperturbed radius of the cylinder while U is the magnitude of the velocity of the fluid sufficiently far from the cylinder. It was taken here to be along the x-axis, such that $\vec{v}=\nabla\varphi(r\to+\infty)=U\vec{e}_x$.

The solution developed here is based on complex analysis and conformal mappings, and has been developed based on [1] [2] [3] [4]. Results from these documents will be used extensively throughout this short work. In the following, for the sake of clarity U was taken equal to 1, without loss of generality.

Solution using conformal mappings

The proposed solution is based on conformal mappings and thus implies switching from the physical space to the conformal space. For the sake of clarity, in the following, the complex variable $\xi\in\mathbb{C}$ will refer to the physical space Ω (where the initial problem is formulated) while the complex variable $z\in\mathbb{C}$ will refer to the conformal space D (namely, that of the regular cylinder).

In the physical space, we are dealing with a *perturbed* cylinder, which can be described by the set of points

$$\xi=r_0(1+\varepsilon\cos(\theta))\exp(i\theta),\ r_0,\epsilon\in\mathbb{R}^+,\ \theta\in[0,2\pi].$$

Note that the variable ξ was used, in agreement with previous remarks.

Riemann's mapping theorem ensures that one can map any simply connected subset of $\mathbb{C}$ to the unitary disk. This is very useful in this problem as the knowledge of a conformal mapping would enable us to transfer the knowledge of the solution around a unitary disk (and thus a regular cylinder) to that around a *perturbed* cylinder. One can use the following holomorphic function (which is then similar to a conformal map at any point where its derivative is non-zero) to map the cylinder $z=r_0\exp(i\theta)$ to the perturbed cylinder:

$$\xi(z)=\frac{\varepsilon}{r_0}z^2+z+\epsilon r_0. \tag{1}$$

This amounts to saying that we can switch back from the conformal space to the physical space with

$$z=\frac{r_0}{2\varepsilon}\left(((r_0+\zeta\epsilon 4i+4\varepsilon\eta-4\varepsilon^2r_0)/r_0)^{1/2}-1\right), \tag{2}$$

where $\xi=\eta+i\zeta,(\eta,\zeta)\in\mathbb{R}^2$. We thus have to solve the problem in the conformal space with appropriate boundary conditions and then translate it back to the physical space.

Finding appropriate boundary conditions

The first boundary condition, which states that no fluid can penetrate the solid, is valid in both spaces Ω and D. Therefore, we have that $\vec{n} \cdot \nabla \varphi = 0$ on ∂D. The condition "far" from the solid, however, is not identical. In the physical space, we want that $\varphi = \eta$ as $|\xi| \to \infty$. Indeed, that amounts to requiring $v = \nabla_\xi \varphi = (1, 0)$ far from the solid, and thus amounts to an unperturbed horizontal flow. Relation (1) enables us to write η as a function of the two axes of the conformal space. Writing $z = x + iy$, we indeed have

$$\eta = \Re(\xi) = \frac{\varepsilon}{r_0}(x^2 - y^2) + x + \varepsilon r_0. \tag{3}$$

Solving in the conformal space

Therefore, we have two boundary conditions. We can now solve in the conformal space the following problem:

$$\begin{aligned}
&\Delta\varphi(z) = 0, z \in D = \{z \in \mathbb{C} : |z| >= 1\} \\
&\vec{n} \cdot \nabla\varphi = 0, \forall z \in \partial D \\
&\varphi = \frac{\varepsilon}{r_0}(x^2 - y^2) + x + \varepsilon r_0, z \to \infty.
\end{aligned}$$

We will now work with polar coordinates in the conformal space, that is $z = x + iy = r\exp(i\theta)$. In those coordinates, we know the general solution to the problem at hand :

$$\phi = A_0 \log(r) + B_0 + \sum_{n\geq 1} \left[A_n \cos(n\theta) + B_n \sin(n\theta)\right] r^n + \sum_{n\geq 1} \left[\tilde{A}_n \cos(n\theta) + \tilde{B}_n \sin(n\theta)\right] r^{-n}. \tag{4}$$

In polar coordinates, the condition at ∞ translates to

$$\varphi = \frac{\varepsilon}{r_0} r^2 \cos(2\theta) + r\cos(\theta) + \varepsilon r_0, r \to \infty. \tag{5}$$

Therefore, this leads us to $A_0 = 0$, $B_0 = \varepsilon r_0$, $A_1 = 1$, $A_2 = \frac{\varepsilon}{r_0}$, $B_{\geq 1} = A_{\geq 3} = 0$. However, nothing can be said regarding $\tilde{A}_n$ and $\tilde{B}_n$. The condition at the boundary of the cylinder simply amounts to $\frac{\partial \varphi}{\partial r}|_{r_0} = 0$. Therefore, we easily have $\tilde{B}_{\geq 1} = \tilde{A}_{\geq 3} = 0$, $\tilde{A}_1 = r_0^2$ and $\tilde{A}_2 = \varepsilon r_0^3$. Therefore, the solution can easily be written in polar coordinates in the conformal space as

$$\varphi = \frac{\varepsilon}{r_0} r^2 \cos(2\theta) + r\cos(\theta) + \varepsilon r_0 + \frac{r_0^2}{r}\cos(\theta) + \frac{\varepsilon r_0^3}{r^2}\cos(2\theta). \tag{6}$$

Switching back to the physical space

Now that the solution has been well-established in the conformal space, we need to recover it in the physical space. As the conformal mapping has been established in cartesian coordinates, one should first translate the derived potential in the (x, y) axes of the conformal space. This is easily done by writing r, θ as functions of x, y which leads to an expression $\varphi(r(x, y), \theta(x, y)) = \varphi(x, y)$.

The solution in the physical space is then obtained by using the conformal transformation. Indeed, we have $x = \Re(z) = x(\eta, \zeta)$ and $y = \Im(z) = y(\eta, \zeta)$. Injecting those values in the expression for the potential yields the solution in the actual space. No closed-form expression of the final solution has been achieved, as it requires tedious and non-interesting calculations.

Results

In order to illustrate and validate the proposed solution, some results are provided here below.

Potential field

Figs. 1 and 2 provide illustrations of both the perturbed cylinder and the equipotential field lines for different values of ε. As can be seen, even for relatively large values of the perturbation parameter, both boundary conditions are still satisfied. On a qualitative standpoint at least, this observation validates the solution.

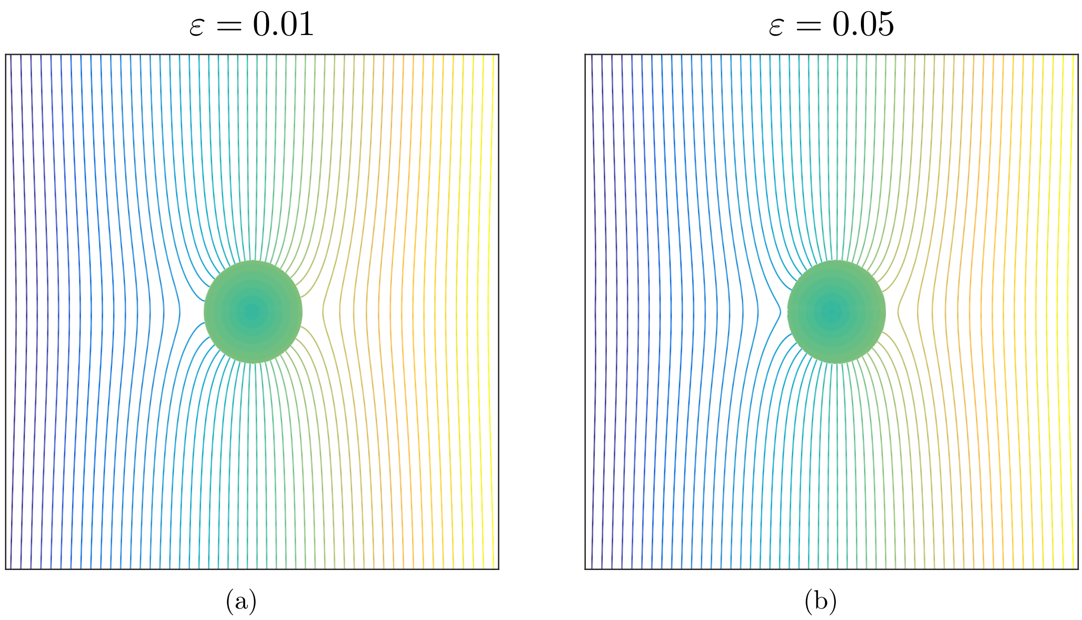

Figure 1 – Perturbed cylinder and equipotential field lines for different values of the perturbation parameter ε, with $r_0 = 1$.

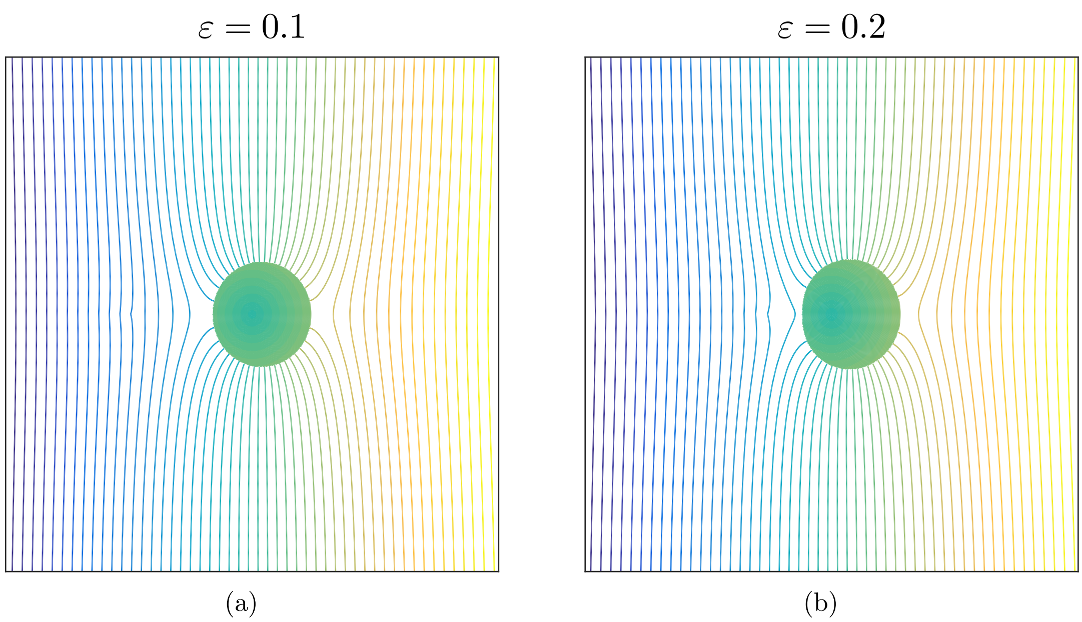

Figure 2 – Perturbed cylinder and equipotential field lines for different values of the perturbation parameter ε, with $r_0 = 1$.

Comparison with estimated solution

In the course, the approximate solution in the physical space has been derived as

$$\varphi = Ur\cos(\theta)\left(1+(\frac{r_0}{r})^2\right)+\varepsilon U r_0\cos(2\theta)(\frac{r_0}{r})^2+O(\varepsilon^2). \tag{7}$$

Note that here the polar coordinates are used in the physical space, that is $\xi = \eta + i\zeta = r\exp(i\theta)$. In order to further validate the solution on a more quantitative standpoint, let us compare both the above estimation (with $U = 1$) and the solution obtained with conformal mappings. Below, φ_{CM} refers to the solution obtained with conformal mappings while φ_{PM} refers to the estimate derived with perturbation methods.

Figs. 3 and 4 provide cuts of the potential field along the η-axis for both solutions, while Figs. 5 and 6 provide cuts of the potential field along the ζ-axis. As can be seen, for small values of ε, both solutions are indistinguishable while this is not the case anymore for larger values of ε.

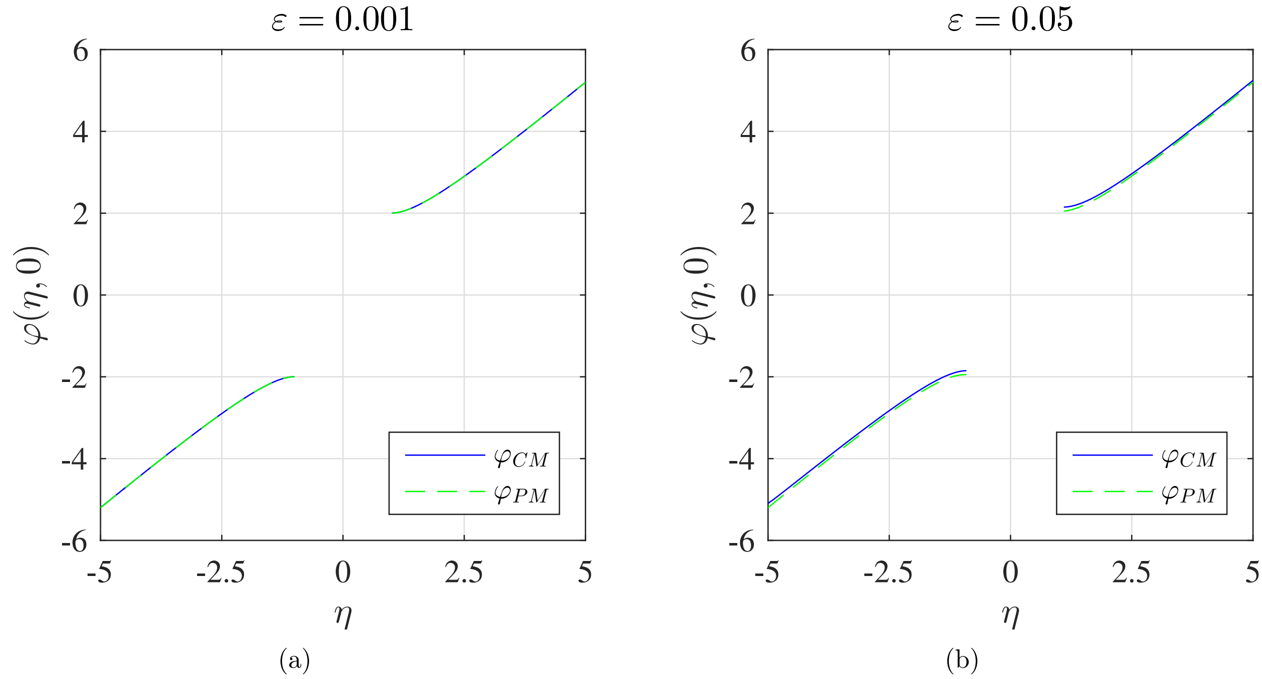

Figure 3 – Potential field along the η-axis. Comparison of both solutions for different values of the perturbation parameter.

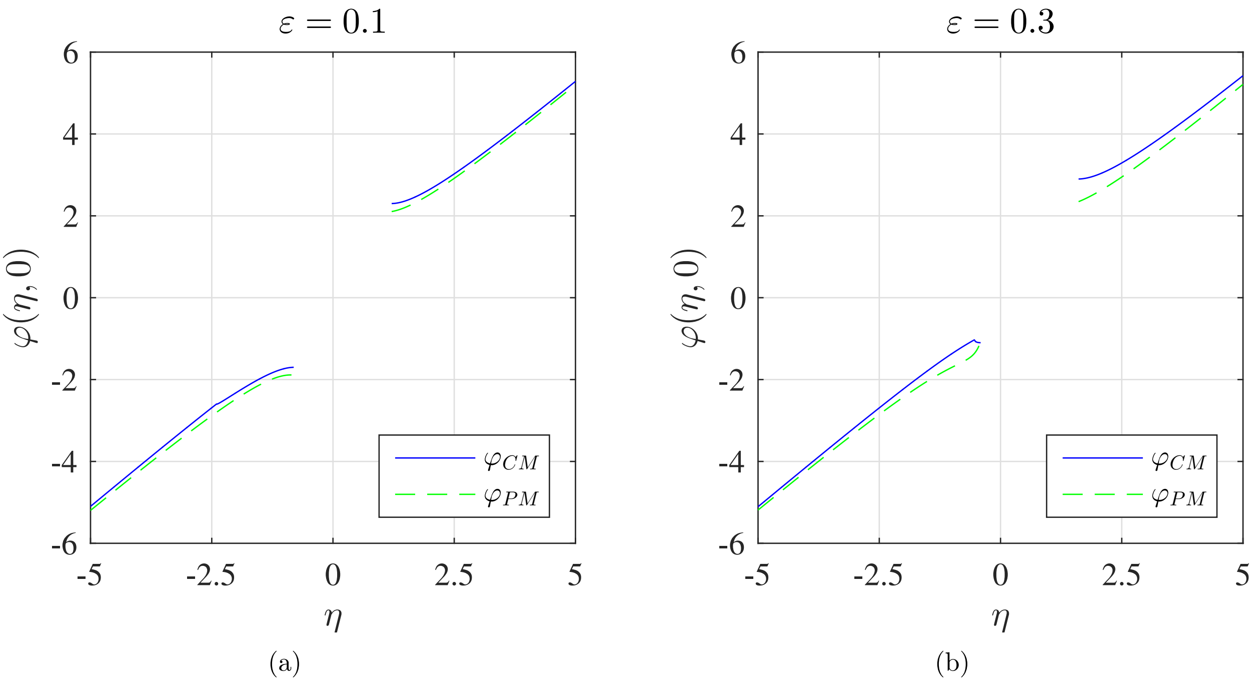

Figure 4 – Potential field along the η-axis. Comparison of both solutions for different values of the perturbation parameter, with $r_0 = 1$.

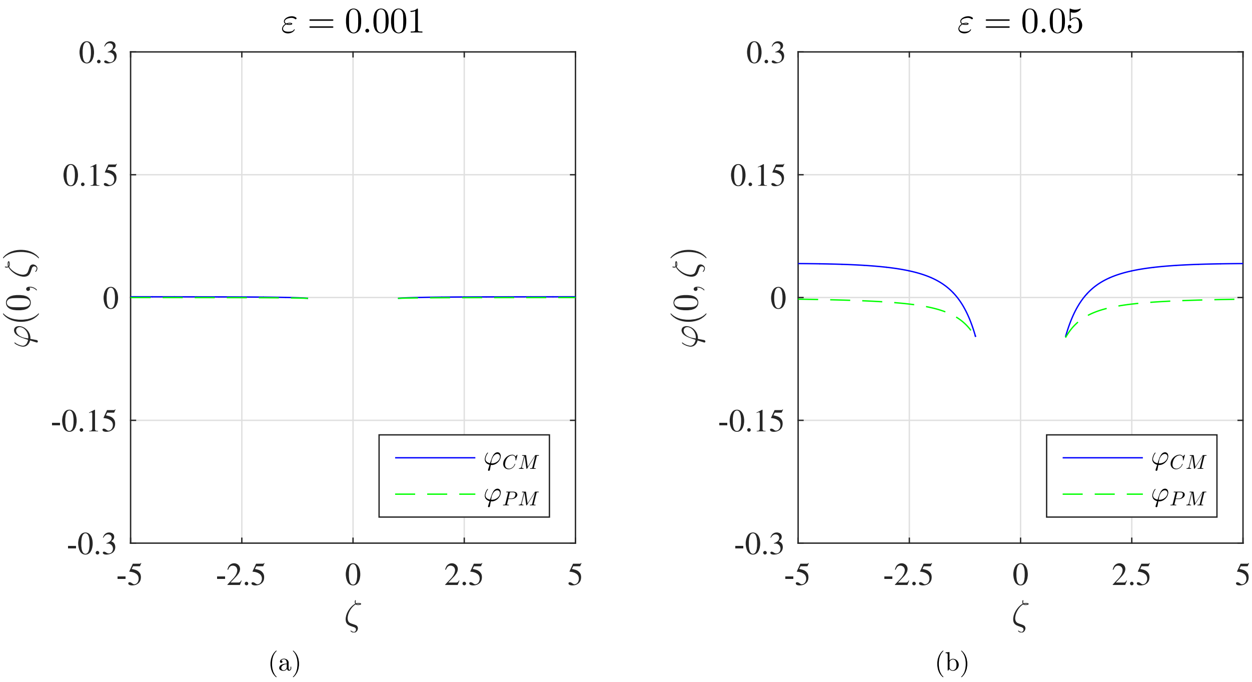

Figure 5 – Potential field along the ζ-axis. Comparison of both solutions for different values of the perturbation parameter, with $r_0 = 1$.

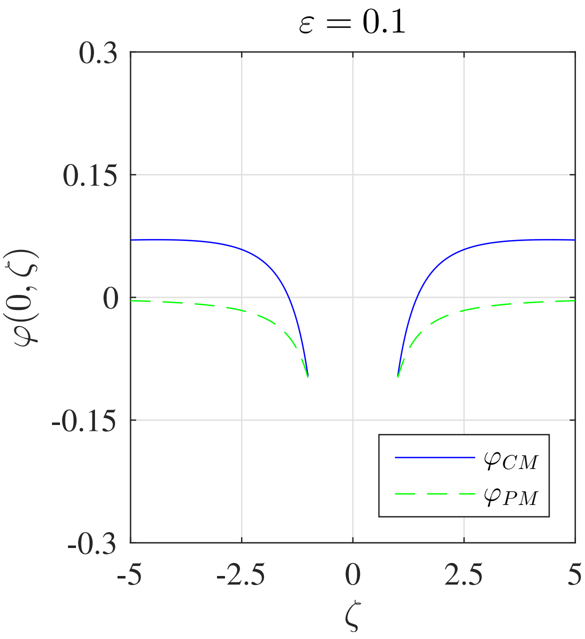

(a)

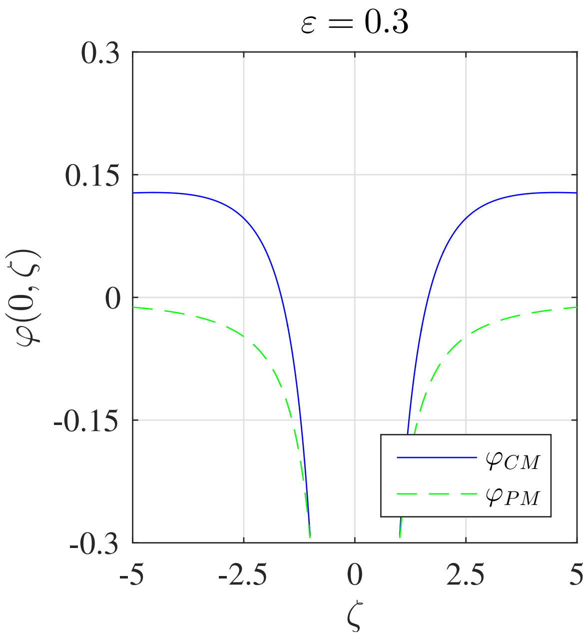

(b)

Figure 6 – Potential field along the ζ-axis. Comparison of both solutions for different values of the perturbation parameter, with $r_0 = 1$.

In order to make it even clearer, Fig. 7 provides a graph of the error on a whole domain for increasing values of ε. The error was defined as

$$\text{Error} = \frac{1}{N_\eta N_\zeta} \sum_{i=1}^{N_\eta} \sum_{j=1}^{N_\zeta} \left(\varphi_{CM}(\eta_i, \zeta_j) - \varphi_{PM}(\eta_i, \zeta_j)\right)^2 , \tag{8}$$

where (η_i, ζ_j) are the grid points at which both functions are evaluated, and N_η, N_ζ are the number of grid points along each axis. As can be seen, the error rises dramatically for values of $\varepsilon > 10^{-2}$. Therefore, one can conclude that the estimated solution is not valid anymore beyond this point.

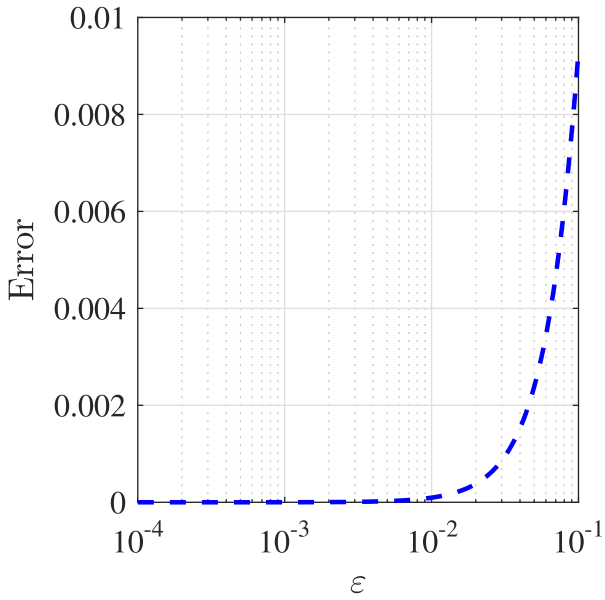

Figure 7 – Error between both solutions on the domain $(\eta, \zeta) \in [-3; 3]^2$, with grid size $5 \cdot 10^{-2}$.

References

[1] Peter J. Olver, Complex Analysis and Conformal Mapping, University of Minnesota

[2] Christophe Ancey, Outils mathématiques pour la dynamique des fluides, Laboratoire Hydraulique Environnementale, EPFL

[3] Emmanuel Plaut, Analyse Complexe, ENSEM

[4] Robert G. Owens, Mécanique des fluides, Notes de cours, Université de Montréal